Observation of a transient reaction intermediate illuminates the mechanochemical cycle of the AAA-ATPase p97

Simon Rydzek[1], Mikhail Shein[1], Pavlo Bielytskyi[1], Anne K. Schütz[1,2*]

[1]Bavarian NMR Center, Department of Chemistry, Technical University of Munich, 85748, Garching, Germany

[2]Institute of Structural Biology, Helmholtz Zentrum München, 85764, Neuherberg, Germany

* anne.schuetz@tum.de

Abstract

The human ATPase p97, also known as valosin containing protein or Cdc48, is a highly abundant AAA+ engine that fuels diverse energy-consuming processes in the human cell. p97 represents a potential target for cancer therapy and its malfunction causes a degenerative disease. Here, we monitor the enzymatic activity of p97 in real time via an NMR-based approach that allows us to follow the steps that couple ATP turnover to mechanical work. Our data identify a transient reaction intermediate, the elusive ADP.P_i nucleotide state, which has been postulated for many ATPases but has so far escaped direct detection. In p97, this species is crucial for the regulation of adenosine triphosphate turnover in the first nucleotide-binding domain. We further demonstrate how the enzymatic cycle is detuned by disease-associated gain-of-function mutations. The high-resolution insight obtained into conformational transitions in both protein and nucleotide bridges the gap between static enzyme structures and the dynamics of substrate conversion. Our approach relies on the close integration of solution- and solid-state NMR methods and is generally applicable to shed light on the mechanochemical operating modes of large molecular engines.

Introduction

p97 powers multiple processes indispensable to the survival of human cells including protein homeostasis[1], chromatin-associated functions[2], cell cycle progression[3], apoptosis[4] and membrane fusion[5]. The role of p97 is that of a molecular motor that segregates, remodels, and unfolds biomolecular complexes[6]. A member of the ATPases Associated with diverse cellular Activities (AAA+) superfamily[7], p97 is a symmetric hexamer formed by two nucleotide binding domains, D1 and D2, assembled into two planar rings, which can adopt a staircase-like arrangement in complex with cofactors as substrates are translocated through the central pore[8-10]. From structures determined by crystallography[11-13] and cryo-electron microscopy (cryo-EM)[14, 15] in the presence of either ATPγS or ADP, high-resolution snapshots of the enzymatic cycle have emerged. The cofactor-binding N-terminal domain (NTD) undergoes a major downward motion between ATPγS- and ADP-bound states of D1[11] (Figure 1a, Figure S1). This motional freedom of the NTD is a prerequisite for enzymatic activity of both D1 and D2[16], the nucleotide states of which appear to be coupled[14, 17]. Beyond controlling NTD motion to generate the major power stroke in p97, the D1 domain also mediates the binding of the majority of cofactors[18]. Meanwhile, D2 accomplishes substrate unfolding[8, 9] and contributes more strongly to the overall ATPase activity of the enzyme[17].

Mechanistic questions remain regarding the operating mode of p97, which we address here for the D1 domain of p97: During which step of the ATP-hydrolysis cycle is mechanical work generated? Which step is rate-limiting? Are there additional reaction intermediates that have not yet been trapped? Is ATP turnover coordinated among the hexamer subunits? How do disease-associated mutations in p97 interfere with the above?

We employed Nuclear Magnetic Resonance (NMR) spectroscopy in solution and in the solid state under magic angle spinning (MAS) to watch the enzyme and its bound nucleotide during live enzymatic activity. By modulating the activity via mutations, we disentangled the underlying kinetics and deduced a mechanochemical cycle for the first nucleotide binding domain of p97.

Results

A transient reaction intermediate limits ATP turnover in p97 D1 domain.

We performed experiments on methyl-labelled full-length p97 (6x806 residues) and a minimal model comprising NTD and D1 (first 6x480 residues, termed ND1L), which is sufficient for the nucleotide-driven domain rearrangement of the NTD[12, 19] and affords NMR data with higher resolution. An ATP regeneration system in the NMR tube[20] (Figure 1a, Figure S2) allowed us to maintain a ratio of ATP to ADP within the physiological range of mammalian cells: low millimolar concentration of free ATP, with ADP ranging from several orders of magnitude lower up to equal concentrations with respect to ATP, depending on cell type and environment[21, 22]. To monitor p97 during ATP turnover and at rest, series of two-dimensional methyl correlation spectra[23] of the protein were acquired over time, first in the presence of pure ATP, then, as the fuel of the regeneration system was depleted, in a mixture of ATP and ADP (Figure 1b). To read out conformational transitions of the enzyme, we had access to 130 assigned methyl probes[19], distributed evenly over residues 1-480 (55 in NTD; 4 in linker; 71 in D1).

The relative populations of different p97 species observed in the NMR spectra reflect the kinetic rates of each step of the enzymatic cycle. In the presence of only ATP (steady state, region I/II in Figure 1b), we detect one correlation per residue (full spectra in Figure S3). Since the NMR chemical shift is a highly sensitive reporter of

protein secondary, tertiary and quaternary structure, the observation of a single correlation for each methyl group implies the existence of a single symmetric species of the homo-oligomeric p97 complex. Since this species is predominant during the steady state, its turnover must be the rate-limiting step of the cycle. The majority of chemical shifts are identical or similar to those of ADP-bound p97 (Figure 1c, red contours, right panel), which is distinct from apo (blue, middle panel) and ATPγS-bound p97 (black, left panel), consistent with a coplanar position of the NTD. However, 20 methyl-bearing amino acid residues display deviations from the ADP-bound form (Figure 1d-e, Figure S4 and Table S1), with a subset shifting towards an ATPγS-like state and others perturbed or obliterated. The effects cluster around the nucleotide binding pocket and radiate outward from the residues critical for nucleotide binding and hydrolysis, the Walker motifs and arginine fingers[24]. Analogous observations were made for the truncated ND1L and full-length wild-type protein (Figure S5a-c). Once the ATP:ADP ratio fell below ~50:1, additional correlations originating from ADP-bound p97 appeared (region III in Figure 1d), and upon depletion of the regeneration system, the spectra completely reverted to the ADP-bound state (region V).

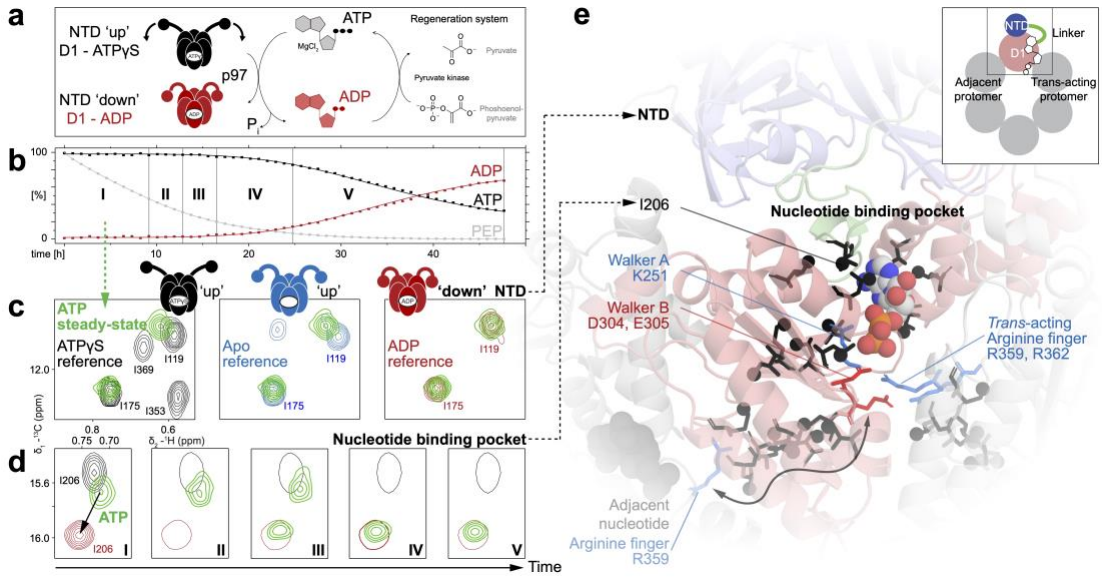

Figure 1. Nucleotide turnover by p97 followed in real time. a. NTD moves downward relative to the hexamer barrel formed by D1 as ATP is hydrolysed into ADP and inorganic phosphate released. Schematic of the reaction cycle taking place in the NMR tube: p97 converts ATP to ADP with $MgCl_2$ as a cofactor. ATP is regenerated from ADP via transfer of a phosphate from phosphoenolpyruvate (PEP) by a pyruvate kinase. **b.** The levels of ATP, ADP and PEP were quantified over time from directly pulsed one-dimensional ^{1}H NMR spectra (Figure S2). The reaction lasts until PEP is depleted. **c.** Superposition of two-dimensional methyl correlation spectra of p97-ND1L under ATP turnover (taken from region I from panel b) compared to arrested nucleotide states. Residues I119 and I175 are located in the NTD and report on its position relative to the hexamer barrel formed by D1. The protein is predominantly found in a conformation similar but not identical to its ADP-bound state. **d.** Isoleucine 206 is positioned within 4 Å of the bound nucleotide and part of the linker connecting NTD and D1. This and 19 more residues are detected in a transient state during ATP turnover, which is distinct from the resting ADP-bound state (Figures S3, S4; Table S1). The arrow illustrates peak movement over time. The corresponding data for full-length p97 are shown in Figure S5. **e.** Methyl groups displaying significant chemical shift changes between p97 in the presence of ADP and under ATP turnover are highlighted as black spheres on the crystal structure of ADP-bound p97 (PDB: 1e32[25]). The structural perturbations localize to the nucleotide binding pocket and the adjacent linker region. Functional residues for nucleotide binding and hydrolysis are highlighted as red and blue sticks. The arrow indicates a potential path for communication of nucleotide occupancy around the D1 ring, connecting to the arginine finger of the adjacent protomer.

The transient reaction intermediate is the ADP.P_i nucleotide state.

The data described above identify a reaction intermediate that displays a coplanar NTD and intact symmetry at the time scale of the NMR chemical shift. The chemical shifts resemble ADP-bound p97 but indicate localized structural deviations in the

nucleotide binding pocket of the D1 domain. We thus sought to determine the identity of its bound nucleotide. We performed solid-state ^{31}P-NMR measurements under MAS to observe its phosphate groups[26, 27]. Under MAS, p97 oligomers are sedimented along with their bound nucleotide but remain in exchange with free nucleotide in the surrounding solution[28, 29]. The protein-bound nucleotide can then be detected in cross-polarization and the free nucleotide in directly pulsed NMR experiments. Both the ATPase reaction and the regeneration system remained active in the sediment with kinetics qualitatively similar to solution-state NMR conditions (Figure S6). In the presence of pure ATP (Figure 2b, Figure S7), which captures the transient p97 species, the bound nucleotide displays two sharp ^{31}P resonances, indicative of two phosphate groups within a well-defined nucleotide conformation and a single chemical environment. Their chemical shifts deviate from the expected value for α-phosphate of ADP/ATP and lie in between the expected values for β-phosphates in ATP and ADP, respectively. The additional broad signal is attributed to a third ^{31}P spin in multiple heterogenous chemical environments, evidenced by multiple peak maxima. Upon depletion of the regeneration system, all these signals disappear and two resonances characteristic of p97-bound ADP appear. We hypothesize that the transient species is a post-hydrolysis reaction intermediate with inorganic phosphate (P_i), although cleaved, still trapped in the binding pocket and the ADP molecule not yet fully reverted to its resting-state conformation. This entails unusual dihedral and bond angles in the phosphate backbone, which are reflected by non-canonical ^{31}P chemical shifts of the two sharp ADP resonances[30, 31]. The trapped nucleotide state would thus correspond to the 'ADP.P_i' state, a transient reaction intermediate postulated for many ATPase enzymes, most prominently discussed for myosin[32, 33], but which has escaped direct transient observation so far. Inside the

nucleotide binding pocket, the P_i ion must be immobilized for the lifetime of the ADP.P_i state (~1 min, see below). Positively charged amino acids in the binding pocket could serve as electrostatic anchors, notably the arginine finger residues[34] (Figure 1e). To corroborate our hypothesis of a trapped phosphate ion, we introduced into ADP-bound p97-ND1L arsenate and vanadate ions[26], which mimic inorganic phosphate due to their similar size, charge and geometry (Figure S8c). Peak doublings are observed for a subset of those residues that also display perturbations under active ATP turnover (Figure S8a-b, Table S2). This finding is consistent with a subpopulation of p97 temporarily enclosing an ADP molecule (Figure S9) plus a vanadate or arsenate ion in the nucleotide binding pocket. Finally, we performed ^{31}P-NMR experiments on ATPγS, the γ-thio-substituted analogue of ATP, in complex with p97 (Figure S10). While the majority of ATPγS bound to p97 as such, a small fraction was hydrolysed, as evidenced by the same spectral pattern as observed for the ADP.P_i state but with the broad, heterogeneous signal shifted downfield by ~30 ppm. This distinct effect results unequivocally from the thio-substitution of the γ-phosphate and proves our hypothesis that this signal originates from inorganic (thio)phosphate and not from a small population of nucleotides in a different binding pose.

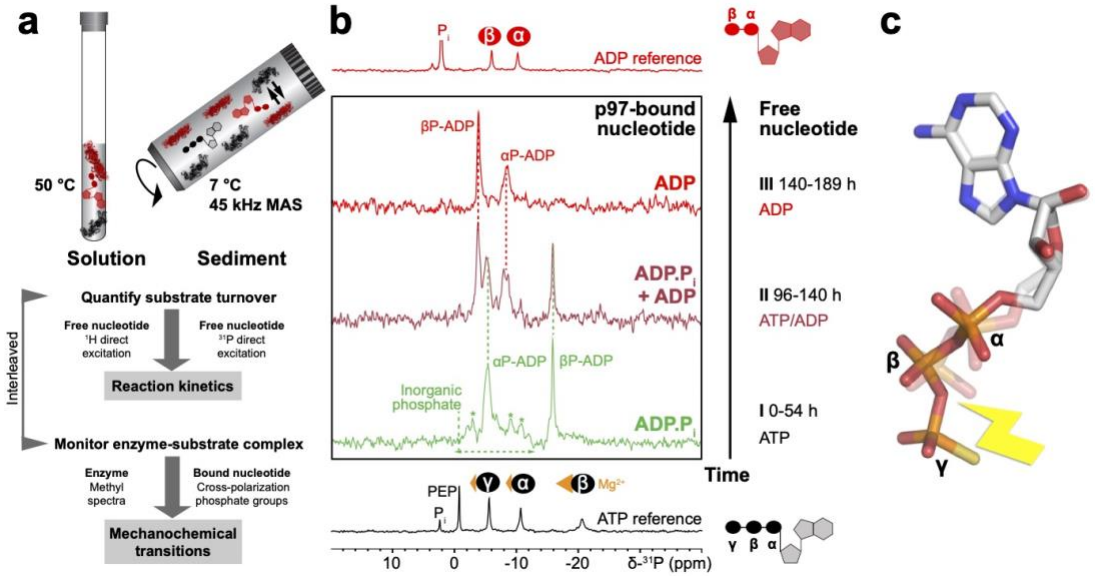

Figure 2. The nucleotide state of the transient reaction intermediate. a. NMR experiments in solution and in the sediment are correlated to monitor simultaneously reaction kinetics and conformational transitions in the protein and its bound nucleotide. **b.** ^{1}H-^{31}P cross-polarization spectra of nucleotide bound to p97 D1 domain acquired over the course of the ATPase reaction. Directly pulsed ^{31}P spectra of ATP (bottom) and ADP (top) in solution are provided for reference with typical chemical shifts indicated for the phosphate groups[26, 35]. Effects of Mg^{2+}-binding on ^{31}P resonances are indicated as orange triangles[35]. **c.** Conformations of ADP and ATPγS when bound to p97 D1 domain (extracted from PDB: 1e32[25] and 4ko8[36]). The bond and dihedral angles in the phosphate backbone differ considerably between the two molecules, consistent with ^{31}P chemical shift changes of several ppm for α- and β-phosphates[30, 31] as the nucleotide changes conformation upon hydrolysis.

Disease-associated mutations deregulate the enzymatic cycle in p97 D1 domain.

Point mutations in p97 associated with degenerative diseases in humans, subsumed under multisystem proteinopathies[37], lead to strongly increased ATPase activity[36, 38, 39]. These mutations cluster at the interface between the NTD and the D1 domain as well as the linker region connecting these domains. The ATPase activities of R95G, R155H and L198W mutants of p97-ND1L were enhanced ~ 20 fold over the wild type under NMR conditions (50 °C to optimise spectral quality; Figures 3a, S11a). At elevated temperatures D1 reaches its peak activity[40] and the effect of disease mutations on the activity of full-length p97 is most pronounced[39]. This activity was too high to sustain constant ATP levels during the acquisition of a two-dimensional

spectrum. From the onset of the reaction, the protein spectra appeared to represent a mixture of p97 in ATPγS- and ADP-like states (Figures S12a-b). We therefore mutated the catalytically active glutamate residue in the Walker B motif in order to reduce the enzymatic activity twentyfold (Figure S11b) and enable NMR analysis of the hyperactive disease-linked mutants. While the E305Q mutation does not affect the spectra of wild-type p97-ND1L under ATP turnover (Figure S5d and explanation in the Materials and Methods), the spectra of the double mutants (E305Q & R155H/L198W/R95G) under ATP turnover show high similarity to those recorded in the presence of ATPγS, with regard both to the upward conformation of the NTD (Figures 3d, S12d) and the D1 domain (Figure 3c). Thus, the pre-hydrolysis, ATP-bound state of p97 is observed, implying that hydrolysis becomes rate-limiting in the disease-associated mutants. Nucleotide-observed spectra confirmed this interpretation with three distinct signals from phosphate groups, indicative of pre-hydrolysis ATP (Figure S13). Meanwhile, the spectral signature of the reaction intermediate could no longer be detected for the disease-associated mutants.

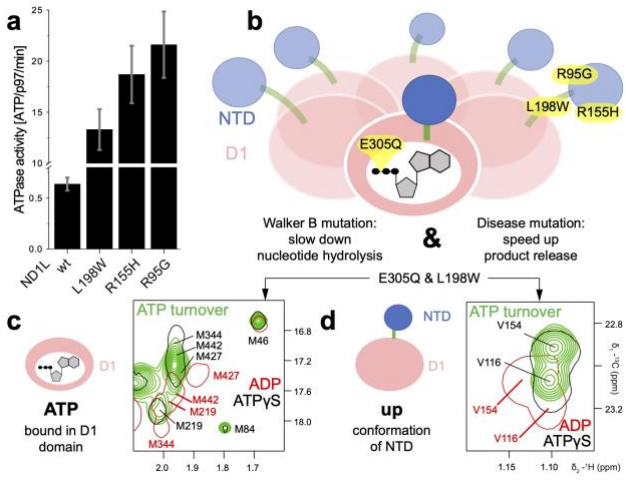

Figure 3. Trapping the pre-hydrolysis form of p97. a. Activities of wild-type p97-ND1L and disease-associated mutants, given in number of ATP molecules hydrolysed per p97 protomer per minute. **b.** Mutations introduced to tune kinetic rates within the enzymatic cycle. **c-d.** Superposition of methyl correlation spectra of p97-ND1L with L198W and E305Q mutations in arrested nucleotide states and under ATP turnover. **c.** The conformation of methionine residues in the D1 domain is similar

to the ATPγS, not the ADP state. **d.** Valine residues located in the NTD indicate its upward position, as in the ATPγS state, not downward as in the ADP and ADP.P_i states. Combined, these findings indicate that p97-ND1L could be trapped pre-hydrolysis (other disease mutants shown in Figure S12).

The active p97 species processes ATP in all six subunits of its D1 ring.

Next, we asked how the presence of ATP/ADP mixtures affects the enzymatic activity of p97. We therefore scrutinized the post steady-state regime (III-V in Figure 1b,d, II-III in Figure S5a,b), where ADP-bound p97 and the ADP.P_i intermediate coexist, both in the full-length and the ND1L construct, as evidenced by the doubling of the correlation of I206. The overall ATPase activity of the reaction system is proportional to the population of the ADP.P_i state (Figure 4a), confirming that this species alone is involved in ATP turnover in the D1 ring while ADP-bound p97 is inactive. We cannot discriminate *a priori* whether ADP and ATP are bound in distinct hexamers, or whether they coexist in the same. However, we noted that the fractions of p97 monomers detected in post-hydrolysis and ADP-bound states do not scale linearly with the proportions of free ATP and ADP in solution, respectively. Already at a ratio of ATP:ADP of ~30:1, a ratio of intermediate versus ADP-bound state of ~2:1 was observed, with analogous findings for the full-length protein (region II in Figure S5b). This implies a thirtyfold higher apparent affinity for ADP over ATP (Figure S14a,b). However, pure ATP and pure ADP bind D1 domain with similar affinities, in the 100 nM range[17, 41], and ATPγS binds even more tightly[12, 36]. This discrepancy can be resolved by invoking coordination of nucleotide binding among subunits within the hexamer. A simple explanation for our observations is that already the binding of one ADP molecule imposes a concerted conformational transition on all protomers and thus locks the whole hexamer in a state that is incompetent to bind ATP or has an overwhelming preference for ADP. Indeed, the experimentally determined

proportions of ADP-bound p97 monomers are in very good agreement with the proportion of hexamers statistically expected to bind at least one ADP molecule (Material and Methods, Figure S14c). Conversely, the prevalence of the ADP.P_i intermediate matches the probability that only ATP is bound within one hexamer. As ATP hydrolysis must precede the ADP.P_i intermediate, the active p97 species must be processing ATP in all six sites in the oligomeric D1 ring – either simultaneously or successively. To obtain a quantitative picture of intra-ring coordination, we tested models assuming either cooperative ADP binding or a symmetry-related hexamer, in which protomers transit in a concerted fashion between up and down conformations of NTD, subject to an ADP-dependent equilibrium (Monod-Wyman-Changeux model[42], MWC). The standard MWC model fits the experimental data (Figure S14d) but only if the competitive binding of ATP is considered, do the fitted affinities approach the experimental ones (Material and Methods, Figure 4b, Table S3).

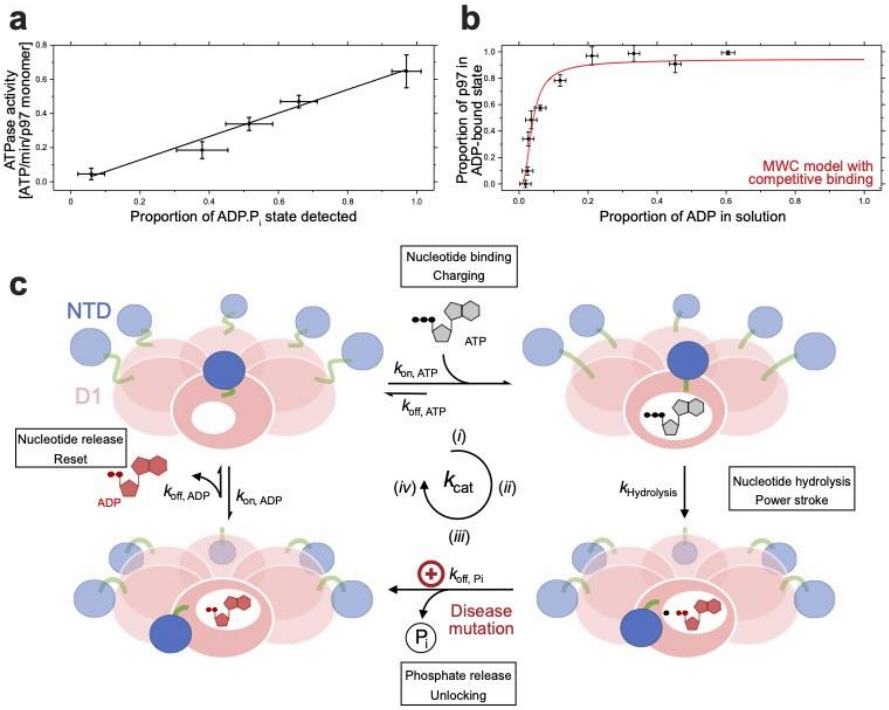

Figure 4. Stepwise model of the mechanochemical cycle within the D1 ring of p97. a. The overall

ATPase activity of the reaction system is proportional to the prevalence of the transient reaction intermediate, identified as the ADP.P_i state. Both quantities were evaluated in regions I-V of the ATPase reaction (Figure 1b,d). **b.** The binding of ADP to the D1 ring of p97 is highly cooperative and can be modelled by a concerted transition according to the Monod-Wyman-Changeux model. The experimental data thus fit best a scenario in which a single ADP molecule in the D1 ring 'locks' the entire hexamer. **c.** The cycle must have at least four intermediates: (*i*) The apo state is rapidly occupied by ATP, which is typically maintained at higher levels than ADP in a functional human cell. (*ii*) Hydrolysis of ATP proceeds fast. It entails a downward motion of NTD with respect to D1. After hydrolysis, the wild-type protein remains in a locked state, in which the D1 nucleotide binding pocket is occupied by ADP.P_i. This is the longest-lived species in the cycle. In disease mutants, this intermediate is inexistent or short-lived, increasing the overall ATP turnover rate. (*iii*) Release of inorganic phosphate is the rate-limiting step of the cycle. (*iv*) The cycle is concluded by the release of ADP, followed by the rapid binding of a new ATP molecule. While the highly cooperative nature of ADP binding to the D1 ring implies that all six subunits in a given hexamer are either collectively at rest or engaged in ATP turnover, we cannot distinguish whether binding and hydrolysis occur in a concerted manner, as depicted here, or via a stochastic, sequential or processive mechanism.

Discussion

We investigated the ATP-hydrolysis cycle of p97 under conditions closely resembling those encountered in the human cell, whereby the enzyme is continuously saturated with its substrate ATP, with ADP typically maintained at significantly lower levels. Figure 4c proposes a model of mechanochemical transitions undergone during the turnover of one ATP molecule in the D1 domain of p97. Estimates of each kinetic rate are given in Table 1.

ND1L construct	**k_{cat} [min^{-1}]**	**$k_{off,Pi}$ [min^{-1}]**	**$k_{hydrolysis}$ [min^{-1}]**	**$k_{on,ADP}$ [min^{-1}]**	**$k_{on,ATP}$ [min^{-1}]**	**$k_{off,ADP}$ [min^{-1}]**	**$k_{off,ATP}$ [min^{-1}]**
wildtype	~1	~1	~20				
Walker B (E305Q)	~0.02	~0.02	~0.04				
Disease mutants	~20	~20	~20	$\gtrsim 8x10^5$	$\gtrsim 6x10^5$	~10-25	~10-25
Disease mutants + Walker B (E305Q)	~0.04	~0.4	~0.04				

Table 1. Estimates of kinetic parameters for the reaction cycle model. Rate-limiting steps highlighted in red determine the overall turnover rate k_{cat}. For disease mutants without mutation in the Walker B motif, nucleotide hydrolysis, phosphate and ADP release could all potentially contribute to limit the reaction speed. The derivation of the kinetic rate constants is explained in detail in the Materials and Methods. Note that the E305Q mutation in the Walker B motif reduces both the rate of phosphate release and the rate of ATP hydrolysis.

The apo state binds ATP rapidly. The NTD is lifted with respect to D1 and assumes a conformation similar to ATPγS-trapped structures. ATP dissociation and hydrolysis occur at similar rates and hence the two processes compete. Hydrolysis of ATP entails a downward motion of the NTD, coupling chemical energy to mechanical work. Next is the two-step product release, initiated by release of inorganic phosphate (P_i). In the wild-type enzyme this step is at least one order of magnitude slower than hydrolysis and rate-limiting for nucleotide turnover in D1. As a result, full-length p97 is enzymatically disabled as locking NTD domain in the down conformation precludes nucleotide turnover in D2[16, 43]. The lifetime of the ADP.P_i state is approximately one minute. Finally, ADP release and binding of a new ATP molecule occur almost simultaneously due to high nucleotide on-rates[17]. In disease mutants, release of P_i proceeds faster and hence ATP turnover is strongly accelerated. Under these conditions, the rate-limiting step becomes ATP hydrolysis. In validation of our model, p97 populations observed by NMR could be shifted between predominantly locked and pre-hydrolysis states by adjusting rate constants via point mutation.

Our study clarifies several open questions regarding the enzymatic cycle of p97. Firstly, it reveals that the hydrolysis of ATP couples chemical and mechanical energy in the form of NTD motion, while the release of P_i is crucial in limiting enzymatic activity of the D1 ring. In other AAA+ proteins, notably the regulatory subunits of the 26S proteasome[44] and ClpXP[45, 46], the release of P_i, not ATP hydrolysis, has been

associated with the most substantial conformational transition or power stroke of the mechanochemical cycle.

Secondly, our study provides the structural rationale for a hypothetical 'locked state', which had been postulated to explain the elevated ATPase activity of p97 disease mutants[12, 36]. In crystal structures, disease mutants feature a peculiar side-chain orientation of the *trans*-acting arginine finger in D1, which is involved in nucleotide binding and inter-subunit communication[47]. We argue that these structural deviations destabilize the 'locked' ADP.P_i state of p97 and promote the premature release of P_i. Indeed, the positively charged R359 residue close to the γ-phosphate of ATP is likely critical in the electrostatic stabilization of the cleaved phosphate ion (Figure 1e). In addition to the structural contribution, there may be a dynamic basis to the altered kinetics of nucleotide release. Previous NMR studies had uncovered a deregulation of inter-domain motions in disease mutants[19, 48], whereby the NTDs undergo a rapid up/down motion with respect to D1 in ADP-bound p97. This manifests in imbalanced cofactor binding to the NTD and accelerated substrate unfolding[49]. It is conceivable that the upward motion of NTD, which is negligible in the wild type but pronounced in disease mutants, may precede or facilitate P_i release as it transiently unlocks the nucleotide binding pocket. Indeed, far-reaching allosteric pathways couple the nucleotide binding pocket and NTD[19]. Conversely, cofactor and substrate binding to NTD could trigger P_i release in D1 and hence unleash a new ATPase cycle when needed[50]. Therefore, future research will address how the ATP-hydrolysis cycle in D1 is modulated in the presence of cofactors.

Thirdly, we contribute to solving the puzzle of how p97 regulates its ATP turnover. Both nucleotide binding domains have similar affinities for ADP and ATP[12, 17, 36, 41], unlike other ATPases, *e.g.* ClpB[51]/Hsp104[52] and Hsp90[53]. Whenever ATP levels

exceed ADP in the cell, p97 would be in idling mode, hydrolysing ATP without processing any protein substrate. One possibility to limit turnover is via the D1-'locked' state, realized via a long-lived reaction intermediate, the ADP.P_i state. From the behaviour of p97 in nucleotide mixtures, we infer a second mechanism whereby ADP can act as competitive inhibitor of ATP, which can tune the activity of p97 when present ~ 10-100 fold below ATP levels and almost fully inhibit at equal ratios, as evidenced by the stalling of the reaction at the end of region V in Figure 1b. A concerted conformational switch of all protomers initiated by the first ADP molecule bound, dictating nucleotide states in neighbour protomers and forcing the whole hexamer into a resting state, could underlie this phenomenon. The observation of 'pre-bound' ADP in purified p97 that cannot be replaced by ATPγS easily[12, 36] could be a manifestation of these ADP-locked hexamers. Our findings are consistent with evidence from native mass spectrometry that nucleotide binding in full-length p97 occurs in discrete cooperative steps of 5–6 nucleotides[15]. For the operating mode of p97, preventing ADP binding to single subunits in D1 could represent a safeguard to prevent futile hydrolysis cycles in which not all subunits of the engine participate. Certain cofactors of p97 could exert their inhibitory effect[5] by breaking the symmetry of the hexamer, hence suppressing cooperativity[47, 54, 55]. Potential routes for communication of nucleotide occupancy around the D1 ring, deduced from structural deviations between ADP and ADP.P_i states, run directly from the Walker residues via the arginine finger to the adjacent nucleotide (Figure 1e). Arginine fingers are conserved across AAA+ proteins and participate in hydrolysis but also nucleotide discrimination and coordination among subunits[24, 56]. In contrast to wild-type p97, the disease mutants are exempt from ADP inhibition (Figure S12a), due to deficiencies in

inter-protomer coordination caused by structural abnormities surrounding the *trans*-acting arginine finger[36] in conjunction with slightly lower affinity for ADP[36, 41].

Finally, p97's mode of action appears to mandate ATP turnover in all six D1 subunits of a given hexamer. Indeed, in NMR spectra of the wild-type protein, the post-hydrolysis reaction intermediate is detected at a level that matches the probability of binding exactly six ATP molecules in one hexamer. A mechanism by which p97 waits for six ATP molecules to bind, hydrolyses all of them and then pauses is conceivable. Subsequently, a coordinated release of P_i and ADP could provide a conformational resetting mechanism that is uniform for all subunits. Alternatively, the mode of operation could be processive in nature, with all subunits remaining engaged in ATP turnover as long as the ADP.P_i intermediate is populated, reminiscent of kinesin[57]. Concerted, sequential or stochastic hydrolysis events are plausible, as long as they proceed fast with respect to the timescale of phosphate release. A transmissive rotary mechanism would fit models of substrate-engaged p97-cofactor complexes which feature a staircase arrangement of protomers in D2[8, 9]. The almost planar arrangement of six, presumably ATP-bound, D1 subunits observed for p97 with cofactor plus substrate[8] integrates very well into our model, whereas the staircase arrangement observed in the presence of nucleotide analogue ADP·BeF_x[8, 9], in which the outermost two subunits are nucleotide-free, is more challenging to reconcile with a symmetric post-hydrolysis ADP.P_i-state. While the p97 engine appears to operate in bursts, the broader AAA+ family harbours mechanistic diversity: coupled ATP hydrolysis but not ADP binding in ClpB[58-60], stochastic hydrolysis paired with coordination among subunits in ClpXP[7, 46, 61, 62] and a sequential mechanism in the ATPase module of the 26S proteasome[44, 63] to name just a few examples.

Conclusion

A transient ADP.P_i-species has not been characterized before at the atomic-level for any ATPase. Our observations for p97 identify challenges associated with the heterogenous environment of the trapped phosphate ion as a possible cause. Transition and ADP.P_i states are often mimicked by inorganic compounds trapped in the nucleotide binding pocket, including vanadate[26, 46], beryllium[9] and aluminium fluoride[11, 27] and exogeneous phosphate[64]. Our integrative NMR approach allows to study and quantitate authentic reactions intermediates, with regard to the conformation of both the nucleotide and its surrounding binding pocket. This provides unique complementary information to recent cryo-EM studies. While the latter have allowed deep structural insight into the working modes of AAA+ enzymes, nucleotide occupancies could not always be unambiguously assigned[8, 44, 65]. We anticipate that our methodology can fill this gap and contribute to resolve the operating modes of other AAA+ proteins and ATPases, GTPases and molecular engines in general.

Materials and Methods

Sample preparation, NMR data acquisition and analysis as well as the calculation of nucleotide occupancies and kinetic parameters are described in the Materials and Methods in the Supporting Information.

Acknowledgement

A.K.S. acknowledges funding from DFG (SCHU3265/1-1), Technical University of Munich, Fonds der Chemischen Industrie, CIPSM DFG cluster EXC114 and the Bavarian NMR Centre. We acknowledge expert advice from Dr. Riddhiman Sarkar on solid-state NMR experiments and technical support from Linda Nguyen.

Competing interests

The authors declare no competing interests.

Associated content

Supporting Information

Materials and Methods with description of sample preparation, NMR data acquisition and evaluation, analysis of kinetics and nucleotide binding; Supporting Figures S1-S14 with illustration of the nucleotide binding pocket, additional NMR spectra, simulations of nucleotide binding; Supporting Tables S1-S5 with tabulated chemical shift perturbations as well as experimental and fitting parameters.

References

1. Richly, H.; Rape, M.; Braun, S.; Rumpf, S.; Hoege, C.; Jentsch, S., A series of ubiquitin binding factors connects CDC48/p97 to substrate multiubiquitylation and proteasomal targeting. *Cell* **2005,** *120* (1), 73-84.
2. Acs, K.; Luijsterburg, M. S.; Ackermann, L.; Salomons, F. A.; Hoppe, T.; Dantuma, N. P., The AAA-ATPase VCP/p97 promotes 53BP1 recruitment by removing L3MBTL1 from DNA double-strand breaks. *Nature Structural & Molecular Biology* **2011,** *18* (12), 1345-U55.
3. Cao, K.; Nakajima, R.; Meyer, H. H.; Zheng, Y. X., The AAA-ATPase Cdc48/p97 regulates spindle disassembly at the end of mitosis. *Cell* **2003,** *115* (3), 355-367.
4. Madeo, F.; Frohlich, E.; Frohlich, K. U., A yeast mutant showing diagnostic markers of early and late apoptosis. *J Cell Biol* **1997,** *139* (3), 729-34.
5. Meyer, H. H.; Kondo, H.; Warren, G., The p47 co-factor regulates the ATPase activity of the membrane fusion protein, p97. *FEBS Lett* **1998,** *437* (3), 255-7.
6. Ye, Y.; Tang, W. K.; Zhang, T.; Xia, D., A Mighty "Protein Extractor" of the Cell: Structure and Function of the p97/CDC48 ATPase. *Front Mol Biosci* **2017,** *4*, 39.
7. Olivares, A. O.; Baker, T. A.; Sauer, R. T., Mechanistic insights into bacterial AAA+ proteases and protein-remodelling machines. *Nat Rev Microbiol* **2016,** *14* (1), 33-44.
8. Twomey, E. C.; Ji, Z. J.; Wales, T. E.; Bodnar, N. O.; Ficarro, S. B.; Marto, J. A.; Engen, J. R.; Rapoport, T. A., Substrate processing by the Cdc48 ATPase complex is initiated by ubiquitin unfolding. *Science* **2019,** *365* (6452), 462-+.
9. Cooney, I.; Han, H.; Stewart, M. G.; Carson, R. H.; Hansen, D. T.; Iwasa, J. H.; Price, J. C.; Hill, C. P.; Shen, P. S., Structure of the Cdc48 segregase in the act of unfolding an authentic substrate. *Science* **2019,** *365*, 502-505.
10. Tonddast-Navaei, S.; Stan, G., Mechanism of transient binding and release of substrate protein during the allosteric cycle of the p97 nanomachine. *J Am Chem Soc* **2013,** *135* (39), 14627-36.
11. DeLaBarre, B.; Brunger, A. T., Complete structure of p97/valosin-containing protein reveals communication between nucleotide domains. *Nature Structural Biology* **2003,** *10* (10), 856-863.
12. Tang, W. K.; Li, D.; Li, C. C.; Esser, L.; Dai, R.; Guo, L.; Xia, D., A novel ATP-dependent conformation in p97 N-D1 fragment revealed by crystal structures of disease-related mutants. *EMBO J* **2010,** *29* (13), 2217-29.
13. Hanzelmann, P.; Schindelin, H., Structural Basis of ATP Hydrolysis and Intersubunit Signaling in the AAA+ ATPase p97. *Structure* **2016,** *24* (1), 127-139.
14. Banerjee, S.; Bartesaghi, A.; Merk, A.; Rao, P.; Bulfer, S. L.; Yan, Y.; Green, N.; Mroczkowski, B.; Neitz, R. J.; Wipf, P.; Falconieri, V.; Deshaies, R. J.; Milne, J. L. S.; Huryn, D.; Arkin, M.; Subramaniam, S., 2.3 Å resolution cryo-EM structure of human p97 and mechanism of allosteric inhibition. *Science* **2016,** *351* (6275), 871-875.
15. Schuller, J. M.; Beck, F.; Lossl, P.; Heck, A. J.; Forster, F., Nucleotide-dependent conformational changes of the AAA+ ATPase p97 revisited. *FEBS Lett* **2016,** *590* (5), 595-604.
16. Niwa, H.; Ewens, C. A.; Tsang, C.; Yeung, H. O.; Zhang, X.; Freemont, P. S., The role of the N-domain in the ATPase activity of the mammalian AAA ATPase p97/VCP. *J Biol Chem* **2012,** *287* (11), 8561-70.
17. Chou, T. F.; Bulfer, S. L.; Weihi, C. C.; Li, K. L.; Lis, L. G.; Walters, M. A.; Schoenen, F. J.; Lin, H. J.; Deshaies, R. J.; Arkin, M. R., Specific Inhibition of p97/VCP ATPase and Kinetic Analysis Demonstrate Interaction between D1 and D2 ATPase Domains. *Journal of Molecular Biology* **2014,** *426* (15), 2886-2899.
18. Buchberger, A.; Schindelin, H.; Hanzelmann, P., Control of p97 function by cofactor binding. *FEBS Lett* **2015,** *589* (19 Pt A), 2578-89.
19. Schuetz, A. K.; Kay, L. E., A Dynamic molecular basis for malfunction in disease mutants of p97/VCP. *Elife* **2016,** *5*, e20143.
20. Mas, G.; Guan, J. Y.; Crublet, E.; Debled, E. C.; Moriscot, C.; Gans, P.; Schoehn, G.; Macek, P.; Schanda, P.; Boisbouvier, J., Structural investigation of a chaperonin in action reveals how nucleotide binding regulates the functional cycle. *Sci Adv* **2018,** *4* (9), eaau4196.
21. Beis, I.; Newsholme, E. A., The contents of adenine nucleotides, phosphagens and some glycolytic intermediates in resting muscles from vertebrates and invertebrates. *The Biochemical journal* **1975,** *152* (1), 23-32.
22. Berg, J.; Hung, Y. P.; Yellen, G., A genetically encoded fluorescent reporter of ATP:ADP ratio. *Nature Methods* **2009,** *6* (2), 161-166.

23. Tugarinov, V.; Hwang, P. M.; Ollerenshaw, J. E.; Kay, L. E., Cross-correlated relaxation enhanced 1H-13C NMR spectroscopy of methyl groups in very high molecular weight proteins and protein complexes. *J. Am. Chem. Soc.* **2003,** *125* (34), 10420-10428.
24. Wendler, P.; Ciniawsky, S.; Kock, M.; Kube, S., Structure and function of the AAA+ nucleotide binding pocket. *Biochim Biophys Acta* **2012,** *1823* (1), 2-14.
25. Zhang, X.; Shaw, A.; Bates, P. A.; Newman, R. H.; Gowen, B.; Orlova, E.; Gorman, M. A.; Kondo, H.; Dokurno, P.; Lally, J.; Leonard, G.; Meyer, H.; van Heel, M.; Freemont, P. S., Structure of the AAA ATPase p97. *Mol Cell* **2000,** *6* (6), 1473-84.
26. Kaur, H.; Abreu, B.; Akhmetzyanov, D.; Lakatos-Karoly, A.; Soares, C. M.; Prisner, T.; Glaubitz, C., Unexplored Nucleotide Binding Modes for the ABC Exporter MsbA. *J Am Chem Soc* **2018,** *140* (43), 14112-14125.
27. Wiegand, T.; Cadalbert, R.; Lacabanne, D.; Timmins, J.; Terradot, L.; Bockmann, A.; Meier, B. H., The conformational changes coupling ATP hydrolysis and translocation in a bacterial DnaB helicase. *Nat Commun* **2019,** *10* (1), 31.
28. Mainz, A.; Jehle, S.; Van Rossum, B. J.; Oschkinat, H.; Reif, B., Large protein complexes with extreme rotational correlation times investigated in solution by magic-angle-spinning NMR spectroscopy. *J Am Chem Soc* **2009,** *131* (44), 15968-15969.
29. Bertini, I.; Luchinat, C.; Parigi, G.; Ravera, E.; Reif, B.; Turano, P., Solid-state NMR of proteins sedimented by ultracentrifugation. *Proc Natl Acad Sci U S A* **2011,** *108* (26), 10396-9.
30. Gorenstein, D. G.; Kar, D., 31-P chemical shifts in phosphate diester monoanions. Bond angle and torsional angle effects. *Biochem Biophys Res Commun* **1975,** *65* (3), 1073-80.
31. Gorenstein, D. G., Dependence of phosphorus-31 chemical shifts on oxygen-phosphorus-oxygen bond angles in phosphate esters. *J Am Chem Soc* **1975,** *97* (4), 898-900.
32. Taylor, E. W.; Lymn, R. W.; Moll, G., Myosin-product complex and its effect on the steady-state rate of nucleoside triphosphate hydrolysis. *Biochemistry* **1970,** *9* (15), 2984-91.
33. Lymn, R. W.; Taylor, E. W., Mechanism of adenosine triphosphate hydrolysis by actomyosin. *Biochemistry* **1971,** *10* (25), 4617-24.
34. Zhang, X.; Wigley, D. B., The 'glutamate switch' provides a link between ATPase activity and ligand binding in AAA+ proteins. *Nat Struct Mol Biol* **2008,** *15* (11), 1223-7.
35. Jaffe, E. K.; Cohn, M., 31P nuclear magnetic resonance spectra of the thiophosphate analogues of adenine nucleotides; effects of pH and Mg2+ binding. *Biochemistry* **1978,** *17* (4), 652-7.
36. Tang, W. K.; Xia, D., Altered Intersubunit Communication Is the Molecular Basis for Functional Defects of Pathogenic p97 Mutants. *Journal of Biological Chemistry* **2013,** *288* (51), 36624-36635.
37. Darvish, D.; Pestronk, A.; Whyte, M.; Kimonis, V. E., Inclusion body myopathy–Paget bone disease–frontotemporal dementia syndrome caused by mutated valosin containing protein. *Nat. Genet.* **2004,** *36* (4), 377-381.
38. Tang, W. K.; Xia, D., Role of the D1-D2 Linker of Human VCP/p97 in the Asymmetry and ATPase Activity of the D1-domain. *Sci Rep* **2016,** *6*, 20037.
39. Halawani, D.; LeBlanc, A. C.; Rouiller, I.; Michnick, S. W.; Servant, M. J.; Latterich, M., Hereditary inclusion body myopathy-linked p97/VCP mutations in the NH2 domain and the D1 ring modulate p97/VCP ATPase activity and D2 ring conformation. *Mol Cell Biol* **2009,** *29* (16), 4484-94.
40. Song, C.; Wang, Q.; Li, C. C., ATPase activity of p97-valosin-containing protein (VCP). D2 mediates the major enzyme activity, and D1 contributes to the heat-induced activity. *J Biol Chem* **2003,** *278* (6), 3648-55.
41. Bulfer, S. L.; Chou, T. F.; Arkin, M. R., p97 Disease Mutations Modulate Nucleotide-Induced Conformation to Alter Protein-Protein Interactions. *ACS Chem Biol* **2016,** *11* (8), 2112-6.
42. Monod, J.; Wyman, J.; Changeux, J. P., On the Nature of Allosteric Transitions: A Plausible Model. *J Mol Biol* **1965,** *12* (1), 88-118.
43. Ye, Y.; Meyer, H. H.; Rapoport, T. A., Function of the p97-Ufd1-Npl4 complex in retrotranslocation from the ER to the cytosol: dual recognition of nonubiquitinated polypeptide segments and polyubiquitin chains. *J Cell Biol* **2003,** *162* (1), 71-84.
44. de la Pena, A. H.; Goodall, E. A.; Gates, S. N.; Lander, G. C.; Martin, A., Substrate-engaged 26S proteasome structures reveal mechanisms for ATP-hydrolysis-driven translocation. *Science* **2018,** *362* (6418).
45. Sen, M.; Maillard, R. A.; Nyquist, K.; Rodriguez-Aliaga, P.; Presse, S.; Martin, A.; Bustamante, C., The ClpXP protease unfolds substrates using a constant rate of pulling but different gears. *Cell* **2013,** *155* (3), 636-646.

46. Rodriguez-Aliaga, P.; Ramirez, L.; Kim, F.; Bustamante, C.; Martin, A., Substrate-translocating loops regulate mechanochemical coupling and power production in AAA+ protease ClpXP. *Nat Struct Mol Biol* **2016,** *23* (11), 974-981.
47. Wang, Q.; Song, C.; Irizarry, L.; Dai, R.; Zhang, X.; Li, C. C., Multifunctional roles of the conserved Arg residues in the second region of homology of p97/valosin-containing protein. *J Biol Chem* **2005,** *280* (49), 40515-23.
48. Huang, R.; Ripstein, Z. A.; Rubinstein, J. L.; Kay, L. E., Cooperative subunit dynamics modulate p97 function. *Proc Natl Acad Sci U S A* **2019,** *116* (1), 158-167.
49. Blythe, E. E.; Gates, S. N.; Deshaies, R. J.; Martin, A., Multisystem Proteinopathy Mutations in VCP/p97 Increase NPLOC4.UFD1L Binding and Substrate Processing. *Structure* **2019,** *27* (12), 1820-1829 e4.
50. Bodnar, N. O.; Kim, K. H.; Ji, Z.; Wales, T. E.; Svetlov, V.; Nudler, E.; Engen, J. R.; Walz, T.; Rapoport, T. A., Structure of the Cdc48 ATPase with its ubiquitin-binding cofactor Ufd1-Npl4. *Nat Struct Mol Biol* **2018,** *25* (7), 616-622.
51. Schlee, S.; Groemping, Y.; Herde, P.; Seidel, R.; Reinstein, J., The chaperone function of ClpB from Thermus thermophilus depends on allosteric interactions of its two ATP-binding sites. *J Mol Biol* **2001,** *306* (4), 889-99.
52. Hattendorf, D. A.; Lindquist, S. L., Analysis of the AAA sensor-2 motif in the C-terminal ATPase domain of Hsp104 with a site-specific fluorescent probe of nucleotide binding. *Proc Natl Acad Sci U S A* **2002,** *99* (5), 2732-7.
53. Prodromou, C.; Roe, S. M.; O'Brien, R.; Ladbury, J. E.; Piper, P. W.; Pearl, L. H., Identification and structural characterization of the ATP/ADP-binding site in the Hsp90 molecular chaperone. *Cell* **1997,** *90* (1), 65-75.
54. Beuron, F.; Dreveny, I.; Yuan, X.; Pye, V. E.; McKeown, C.; Briggs, L. C.; Cliff, M. J.; Kaneko, Y.; Wallis, R.; Isaacson, R. L.; Ladbury, J. E.; Matthews, S. J.; Kondo, H.; Zhang, X.; Freemont, P. S., Conformational changes in the AAA ATPase p97-p47 adaptor complex. *EMBO J* **2006,** *25* (9), 1967-76.
55. Zhang, X. Y.; Gui, L.; Zhang, X. Y.; Bulfer, S. L.; Sanghez, V.; Wong, D. E.; Lee, Y.; Lehmann, L.; Lee, J. S.; Shih, P. Y.; Lin, H. J.; Iacovino, M.; Weihl, C. C.; Arkin, M. R.; Wang, Y. Z.; Chou, T. F., Altered cofactor regulation with disease-associated p97/VCP mutations. *Proc Natl Acad Sci U S A* **2015,** *112* (14), E1705-E1714.
56. Ogura, T.; Whiteheart, S. W.; Wilkinson, A. J., Conserved arginine residues implicated in ATP hydrolysis, nucleotide-sensing, and inter-subunit interactions in AAA and AAA+ ATPases. *Journal of structural biology* **2004,** *146* (1-2), 106-112.
57. Milic, B.; Andreasson, J. O. L.; Hancock, W. O.; Block, S. M., Kinesin processivity is gated by phosphate release. *Proceedings of the National Academy of Sciences of the United States of America* **2014,** *111* (39), 14136-14140.
58. Werbeck, N. D.; Schlee, S.; Reinstein, J., Coupling and dynamics of subunits in the hexameric AAA+ chaperone ClpB. *J Mol Biol* **2008,** *378* (1), 178-90.
59. Zeymer, C.; Fischer, S.; Reinstein, J., trans-Acting Arginine Residues in the AAA+ Chaperone ClpB Allosterically Regulate the Activity through Inter- and Intradomain Communication. *Journal of Biological Chemistry* **2014,** *289* (47), 32965-32976.
60. Yamasaki, T.; Oohata, Y.; Nakamura, T.; Watanabe, Y.-h., Analysis of the Cooperative ATPase Cycle of the AAA+ Chaperone ClpB from Thermus thermophilusby Using Ordered Heterohexamers with an Alternating Subunit Arrangement. *The Journal of biological chemistry* **2015,** *290* (15), 9789-9800.
61. Iosefson, O.; Nager, A. R.; Baker, T. A.; Sauer, R. T., Coordinated gripping of substrate by subunits of a AAA+ proteolytic machine. *Nature Chemical Biology* **2015,** *11* (3), 201-206.
62. Cordova, J. C.; Olivares, A. O.; Shin, Y.; Stinson, B. M.; Calmat, S.; Schmitz, K. R.; Aubin-Tam, M. E.; Baker, T. A.; Lang, M. J.; Sauer, R. T., Stochastic but highly coordinated protein unfolding and translocation by the ClpXP proteolytic machine. *Cell* **2014,** *158* (3), 647-58.
63. Wehmer, M.; Rudack, T.; Beck, F.; Aufderheide, A.; Pfeifer, G.; Plitzko, J. M.; Förster, F.; Schulten, K.; Baumeister, W.; Sakata, E., Structural insights into the functional cycle of the ATPase module of the 26S proteasome. *Proc Natl Acad Sci U S A* **2017,** *114* (6), 1305-1310.
64. Wilbanks, S. M.; McKay, D. B., How potassium affects the activity of the molecular chaperone Hsc70. II. Potassium binds specifically in the ATPase active site. *J Biol Chem* **1995,** *270* (5), 2251-7.
65. Majumder, P.; Rudack, T.; Beck, F.; Danev, R.; Pfeifer, G.; Nagy, I.; Baumeister, W., Cryo-EM structures of the archaeal PAN-proteasome reveal an around-the-ring ATPase cycle. *Proc Natl Acad Sci U S A* **2019,** *116* (2), 534-539.

1

2

1 **TOC Figure**

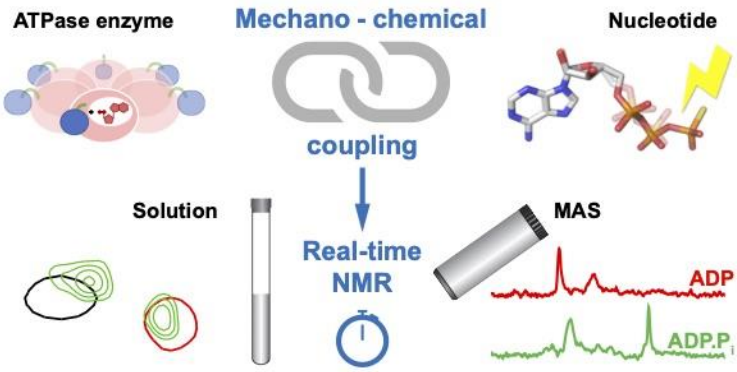

2

3